

# Analysis of GaN MagFETs compatible with RF power technology

Faramehr, S., Thomas, B., Jankovic, N., Evans, J., Elwin, M. & Igic, P.

**Author post-print (accepted) deposited by Coventry University's Repository**

**Original citation & hyperlink:**

Faramehr, S, Thomas, B, Jankovic, N, Evans, J, Elwin, M & Igic, P 2018, Analysis of GaN MagFETs compatible with RF power technology in 41st International Convention on Information and Communication Technology, Electronics and Microelectronics (MIPRO). IEEE, pp. 0050-0053.  
<https://dx.doi.org/10.23919/MIPRO.2018.8400010>

DOI 10.23919/MIPRO.2018.8400010

ISBN 978-953-233-095-3

Publisher: IEEE

**© 2018 IEEE. Personal use of this material is permitted. Permission from IEEE must be obtained for all other uses, in any current or future media, including reprinting/republishing this material for advertising or promotional purposes, creating new collective works, for resale or redistribution to servers or lists, or reuse of any copyrighted component of this work in other works.**

**Copyright © and Moral Rights are retained by the author(s) and/ or other copyright owners. A copy can be downloaded for personal non-commercial research or study, without prior permission or charge. This item cannot be reproduced or quoted extensively from without first obtaining permission in writing from the copyright holder(s). The content must not be changed in any way or sold commercially in any format or medium without the formal permission of the copyright holders.**

**This document is the author's post-print version, incorporating any revisions agreed during the peer-review process. Some differences between the published version and this version may remain and you are advised to consult the published version if you wish to cite from it.**

# Analysis of GaN MagFETs Compatible with RF Power Technology

S. Faramehr\*, B. R. Thomas\*, N. Janković\*\*, J. E. Evans\*\*\*, M. P. Elwin\*\*\* and P. Igić\*

\* Electronic Systems Design Centre (ESDC), College of Engineering, Swansea University, Swansea SA1 8EN, UK

\*\* Microelectronics Department, Faculty of Electronic Engineering, University of Nis, 18000 Nis, Serbia

\*\*\* Centre for NanoHealth (CNH), College of Engineering, Swansea University, Swansea SA2 8PP, UK  
soroush.faramehr@swansea.ac.uk

**Abstract** - The three-dimensional simulations, calibration, measured currents and calculated relative sensitivities of the first-ever fabricated double-drain gallium nitride (GaN) magnetic field effect transistor (MagFET) are given in this work. The MagFETs are GaN high electron mobility transistors (HEMTs) capable of operating under harsh environments. Geometrical and operational analysis are carried out on MagFETs using commercial simulation software Silvaco. The analysis shows promising relative sensitivities of  $6.84\%T^{-1}$  and  $5.04\%T^{-1}$  at ambient temperatures of 400 K and 500 K, respectively. In addition, the relative sensitivity of fabricated device is improved from  $12\%T^{-1}$  to  $24\%T^{-1}$  at 300 K by optimising device geometrical parameters.

**Keywords** - GaN; HEMT; MagFET

## I. INTRODUCTION

In modern power electronics, additional circuitries are added to sense the current passing through the components and to provide system safety. It is a major advantage if the sensor can operate close to the analysed systems under high temperatures and high radiations and provide accurate outputs.

Most of the sensor technologies available in the market are silicon based. Compound semiconductors such as GaN are better candidates for operation under harsh environment. GaN-based devices have proven to be a promising replacement for silicon technology in RF and power applications [1], [2]. The large bandgap, good thermal conductivity, and polarization properties provide various advantageous over the conventional semiconductors. Due to significant interest in electrical and thermal properties of GaN material, commercialization of nitride-based devices is emerging quickly.

It is known that magnetic fields deflect the moving charge in semiconductors and the inversion layer of metal oxide semiconductor field effect transistors (MOSFETs) as reported in previous works [3], [4]. The magnetic field effects in the electronic device can be detected by sensing contacts across the device measuring Hall voltage or by split contacts measuring current imbalance, for instance.

In order to detect the current imbalance resulting from magnetic field, the drain contact is divided into two individual contacts held at the same potential and

separated by a distance (see Fig.1). Ideally, under no magnetic fields, corner contacts on the device with the same length and width will receive equal current flow. In this case, the current difference will be zero and consequently the sensitivity. In the presence of magnetic fields, applied perpendicular to the device surface, the charged carriers are deflected as a result of the Lorentz force. This imbalance can be measured on contacts and the relative sensitivity of the double-drain sensor is calculated by the following equation [5]:

$$S_r[\%T^{-1}] = \frac{|I_{D1} - I_{D2}|}{(I_{D1} + I_{D2}) \times |B|} \times 100\% \quad (1)$$

where  $I_{D1}$  and  $I_{D2}$  are the currents from drain 1 and drain 2 contacts, respectively, in the presence of magnetic field ( $B$ ). The relative sensitivity of split-current sensors may show poor values as the current imbalance is small compared to device total current. Higher sensitivities can be achieved by adding a 3<sup>rd</sup> drain [6] and modifying the magnitude of the current flowing through it. The sensitivity is also a function of geometric parameters as seen in the following equation [7]:

$$S_r = G\mu^* \frac{L}{W} \quad (2)$$

where  $G$  is the geometrical correction factor,  $\mu^*$  is the Hall mobility,  $L$  is the device length and  $W$  is the device width. The Hall electron mobility reads:

$$\mu_n^* = r_n \mu_n \quad (3)$$

where  $r_n$  is Hall electron scattering factor and  $\mu_n$  is effective electron mobility. Furthermore, the current deflection ( $d$ ) is a function of [8]:

$$d = f(L, \mu_n, B, T) \quad (4)$$

where  $L$  is the device length,  $\mu_n$  is the electron mobility,  $B$  is the applied magnetic field and  $T$  is the temperature. To increase the current deflection and relative sensitivity, a

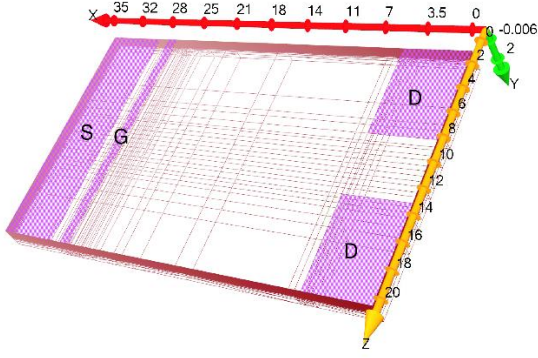


Fig. 1. 3D simulated GaN MagFET showing mesh profile at the device surface and dimensions (in microns) of fabricated device.

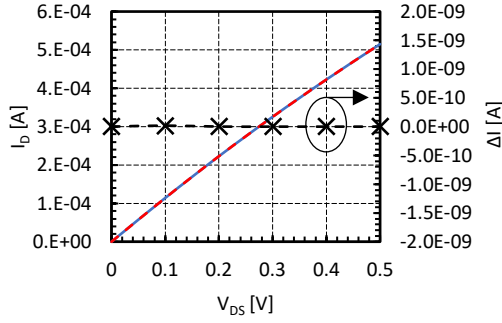


Fig. 2. Simulated drain currents (overlaid) of GaN MagFET ( $I_D$ ) against drain to source voltage ( $V_{DS}$ ) at  $V_{GS}=0V$  and 300 K. The current imbalance ( $\Delta I$ ) is nearly zero in absence of magnetic field ( $B=0$  T).

longer sensor, higher electron mobility, larger magnetic field and lower operational temperature are required. Two-dimensional electron gas (2DEG) channel of GaN hetero-structure fulfils the requirement for high mobility.

The magnetic sensors are integrated with other electronics in the same IC batch to detect magnetic fields in the range of few milli-Tesla.

In this paper, we present simulation, calibration, analysis and optimisation of first-ever fabricated double-drain GaN magnetic sensors. The relative sensitivities and current differences are computed for different geometrical parameters, ambient temperatures and biasing conditions. The simulations are carried out to optimise the GaN device relative sensitivity for integration with a coil to be placed on top of the sensor in micro-meter distance. The current to be sensed flows through the coil producing the magnetic field invoking current imbalance in the GaN device.

## II. DEVICE STRUCTURE AND SIMULATION MODELS

The simulated unintentionally doped (UID) gated sensor is GaN/ $Al_xGa_{1-x}N$ /GaN hetero-structure similar to GaN high electron mobility transistors (HEMTs) on silicon substrate. The mole fraction is  $x=0.25$ . The cap, the barrier, and the buffer thicknesses are 2 nm, 25 nm and 2  $\mu m$ , respectively. The simulated sensor has a source length of  $L_S=5.5 \mu m$ , drain length of  $L_D=5.5 \mu m$ , source width of  $W_S=20 \mu m$ , source to drain distance of  $L_{SD}=24 \mu m$ , source to gate distance of  $L_{GS}=1.0 \mu m$  and gate to drain distance

of  $L_{GD}=22 \mu m$ . The gate contact length is  $L_G=1.0 \mu m$ . The length and width of fabricated/simulated sensors are  $L=35 \mu m$  and  $W=20 \mu m$ , respectively. The separation between two drain contacts is  $L_{DD}=5 \mu m$ . The SiN passivation thickness is  $t_{SiN}=10$  nm.

The spontaneous and piezoelectric polarizations are active in all simulations and the electron sheet density is set to  $9.5 \times 10^{12} \text{ cm}^{-2}$  via polarization adjustments. The unintentional impurities resulting from epitaxial growth are added to the model in GaN:UID buffer at  $E_C-E_T=0.11$  eV and  $E_C-E_T=3.28$  eV [9]. Nitride parameters used in this paper are extracted from the literature [10]. The Shockley-Read-Hall (SRH) and Fermi-Dirac statistics are activated for all simulations. Nitride mobility models for low and high electric fields are employed in 3D simulations. The mobility is considered as effective to account for scattering mechanisms in fabricated device. Self-heating effects are neglected.

The Lorentz force and magnetic effects are modelled using 3D MAGNETIC module of Silvaco atlas. The GaN Hall scattering factor is extracted from the literature [11] and is set to be  $r = 1.1$  in simulations. The magnetic field ( $B$ ) is applied perpendicular to the surface in units of Tesla.

## III. GAN MAGFET SIMULATION AND MEASUREMENT RESULTS

The GaN split-current magnetic sensor with two drains is presented in Fig. 1. The drain contacts have the same length and width to avoid undesirable current offset in the absence of magnetic field.

Fig. 2 shows the output characteristics of the GaN split current sensor in the absence of magnetic field at 300 K. The current flows equally into two drains and the current imbalance ( $\Delta I$ ) is nearly zero for  $V_{DS}=0V$  to  $V_{DS}=0.5V$  at  $V_{GS}=0V$ . The negligible current offset is important to ensure accuracy of simulation results since poor meshing may cause current deflection in absence of magnetic fields.

Fig. 3 is the simulated current imbalance for various applied magnetic fields at  $V_{GS}=0V$ ,  $V_{DS}=0.5V$  and 300 K. The measurements were carried out on 60 fabricated devices and standard deviation resulting from imperfection

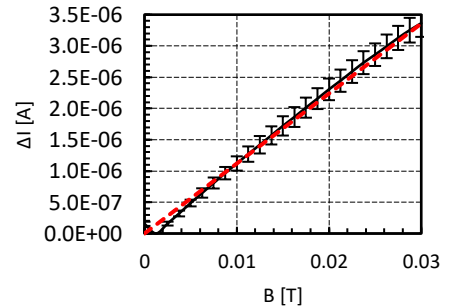


Fig. 3. Simulated current difference ( $\Delta I$ ) of GaN MagFET (dashes) from  $B=0$  T to  $B=0.03$  T in steps of 0.01 T at  $V_{DS}=0.5V$ ,  $V_{GS}=0V$  and 300 K against measured current imbalance (line) in fabricated GaN sensors. The errors bars are calculated standard deviation from 60 fabricated devices. The calculated relative sensitivity is  $S_1=12\%T^{-1}$ .

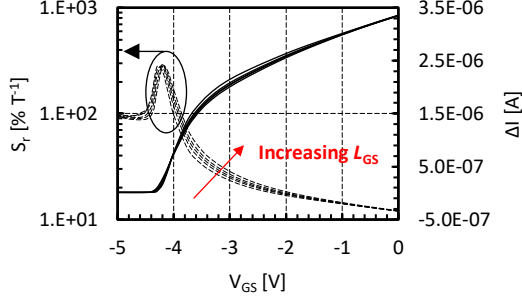


Fig. 4. Simulated relative sensitivities ( $S_r$ ) (dashes) and current difference ( $\Delta I$ ) (lines) of GaN MagFETs for different gate to source spacings of 1.0  $\mu\text{m}$  to 5.0  $\mu\text{m}$  in steps of 1.0  $\mu\text{m}$  where gate length and source to drain spacing is kept constant ( $L_G=1.0 \mu\text{m}$  and  $L_{SD}=24 \mu\text{m}$ ) at  $B=0.03 \text{ T}$ ,  $V_{DS}=0.5 \text{ V}$ , and 300 K.

in fabrication process, geometrical errors and non-uniformity in material resistivity and thickness have been presented with bars. The current difference obtained from simulations has been calibrated to experimental data showing a good agreement.

Fig. 4 is the predicted current imbalance and relative sensitivities for various gate to source spacing of  $L_{GS}=1.0 \mu\text{m}$  to  $L_{GS}=5.0 \mu\text{m}$  in steps of 1.0  $\mu\text{m}$ . Gate length and source to drain spacing are kept constant at  $L_G=1.0 \mu\text{m}$ ,  $L_{SD}=24 \mu\text{m}$ , respectively. Due to reduction in total current [12] of the device and increase in the Lorentz force between gate and drain resulting from this scaling, simulation results show increase in relative sensitivities. This effect is more pronounced at low gate biases. It needs to be mentioned that keeping the device length constant and scaling up the gate to source distance may trigger impact ionisation at lower biasing conditions [13].

Fig. 5 is the simulated differential current and relative sensitivities for different gate lengths of  $L_G=1.0 \mu\text{m}$  to  $L_G=5.0 \mu\text{m}$  in steps of 1.0  $\mu\text{m}$  where gate to source and source to drain spacings are kept constant at  $L_{GS}=1.0 \mu\text{m}$  and  $L_{SD}=24 \mu\text{m}$ , respectively. Scaling up the gate length

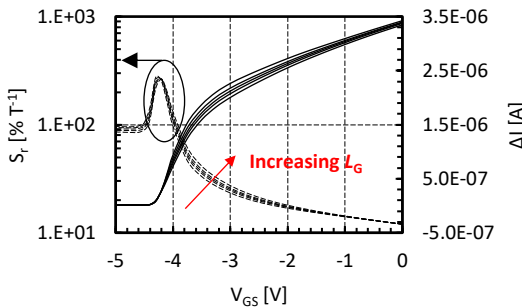


Fig. 5. Simulated relative sensitivities ( $S_r$ ) (dashes) and current difference ( $\Delta I$ ) (lines) of GaN MagFETs for different gate lengths of 1.0 to 5.0  $\mu\text{m}$  in steps of 1.0  $\mu\text{m}$  where the gate to source and source to drain spacings are kept constant ( $L_{GS}=1.0 \mu\text{m}$  and  $L_{SD}=24 \mu\text{m}$ ) at  $B=0.03 \text{ T}$ ,  $V_{DS}=0.5 \text{ V}$ , and 300 K.

reduces the device total current [12]. Consequently, improvement in relative sensitivity is observed. In addition, increase in the electric field resulting from this scaling between gate and drain is also predicted.

Fig. 6 is the simulated current difference and calculated relative sensitivities at  $V_{DS}=0.5 \text{ V}$ , 300 K and various ambient temperatures. The simulation predicts promising relative sensitivities of  $S_r=6.84\% \text{ T}^{-1}$  and  $S_r=5.04\% \text{ T}^{-1}$  at high temperatures of 400 and 500 K compared to  $S_r=12\% \text{ T}^{-1}$  at 300 K. The degradation is due to electron mobility and velocity reduction [14], [15]. Moreover, threshold voltage shift is also observed from TCAD results due to trap states at the device surface [16].

Fig. 7 is the comparison between the optimised device ( $L=65 \mu\text{m}$ ,  $W=20 \mu\text{m}$ ,  $L_S=5.5 \mu\text{m}$ ,  $W_S=5.0 \mu\text{m}$ ,  $L_{DD}=5 \mu\text{m}$ ,  $L_G=5.0 \mu\text{m}$  and  $L_{GD}=10 \mu\text{m}$ ) against the sensor with  $L=35 \mu\text{m}$ ,  $W=20 \mu\text{m}$ ,  $L_S=5.5 \mu\text{m}$ ,  $W_S=20 \mu\text{m}$ ,  $L_{DD}=5 \mu\text{m}$ ,  $L_G=1.0 \mu\text{m}$  and  $L_{GD}=22 \mu\text{m}$ . An increase in sensitivity (from  $S_r=12\% \text{ T}^{-1}$  to  $S_r=24\% \text{ T}^{-1}$ ) is predicted at  $V_{GS}=0 \text{ V}$  for the optimised GaN magnetic sensor. The increase in relative sensitivity at  $V_{GS}=0 \text{ V}$  is mainly due to increase of source to drain resistance and reduction of total current, while at low gate biases is also due to increase in current imbalance resulting from a larger Lorentz force.

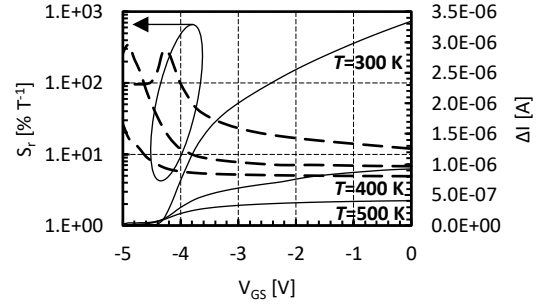


Fig. 6. Simulated relative sensitivity ( $S_r$ ) (dashes) and current difference ( $\Delta I$ ) (lines) of GaN MagFET for different ambient temperatures of  $T=300 \text{ K}$ ,  $T=400 \text{ K}$  and  $T=500 \text{ K}$  at  $V_{DS}=0.5 \text{ V}$  and  $B=0.03 \text{ T}$ .

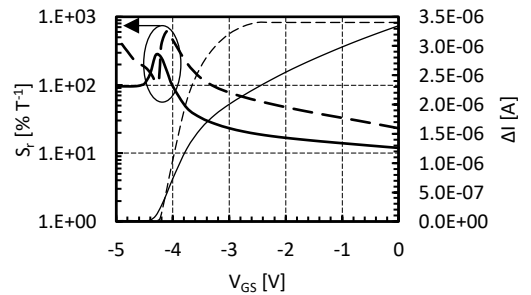


Fig. 7. Simulated relative sensitivity ( $S_r$ ) (dash) and current difference ( $\Delta I$ ) (dash) of optimised GaN MagFET ( $L=65 \mu\text{m}$ ,  $W=20 \mu\text{m}$ ,  $L_S=5.5 \mu\text{m}$ ,  $W_S=5.0 \mu\text{m}$ ,  $L_{DD}=5 \mu\text{m}$ ,  $L_G=5.0 \mu\text{m}$  and  $L_{GD}=10 \mu\text{m}$ ) against previously simulated GaN MagFET relative sensitivity (line) and current difference (line) with  $L=35 \mu\text{m}$ ,  $W=20 \mu\text{m}$ ,  $L_S=5.5 \mu\text{m}$ ,  $W_S=20 \mu\text{m}$ ,  $L_{DD}=5 \mu\text{m}$ ,  $L_G=1.0 \mu\text{m}$  and  $L_{GD}=22 \mu\text{m}$  at  $V_{DS}=0.5 \text{ V}$  and 300 K.

#### IV. CONCLUSION

Three-dimensional simulations have been employed to study relative sensitivities, the main figure of merit of magnetic sensors. Simulated current difference was calibrated against measured data to validate simulations obtained from Silvaco software. Geometrical analysis was carried out on GaN split-current magnetic sensor demonstrating increase in relative sensitivities with scaling up the gate length and source to gate spacing. We also presented an optimised device predicting an increase in relative sensitivity from  $S_r=12\%T^{-1}$  to  $S_r=24\%T^{-1}$  at  $V_{GS}=0V$ ,  $V_{DS}=0.5V$  and 300 K. In addition, three dimensional simulations were carried out to study the relative sensitivities at 300 K, 400 K and 500 K ambient temperatures predicting a promising operation of GaN split-current sensors under harsh environment.

#### ACKNOWLEDGMENT

This work was supported by FLEXIS, the European Regional Development Fund through the Welsh Government. We would like to thank industrial collaborators, Compound Semiconductor Centre (CSC) and IQE Europe Limited in Cardiff, Wales for providing us with GaN hetero-structures for MagFETs fabrication at Swansea University.

#### REFERENCES

- [1] S. Faramehr, K. Kalna, and P. Igić, "Drift-diffusion and hydrodynamic modeling of current collapse in GaN HEMTs for RF power application," *Semicond. Sci. Technol.*, vol. 29, no. 2, pp. 025007-025017, Jan. 2014.
- [2] S. Faramehr, K. Kalna, and P. Igić, "Design and simulation of a novel 1400 V–4000 V enhancement mode buried gate GaN HEMT for power applications," *Semicond. Sci. Technol.*, vol. 29, no. 11, pp. 115020-115026, Sep. 2014.
- [3] A. C. Beer, "The Hall effect and related phenomena," *Solid. State. Electron.*, vol. 9, no. 5, pp. 339–351, May 1966.
- [4] R. C. Gallagher and W. S. Corak, "A Metal-Oxide-Semiconductor (MOS) Hall element," *Solid. State. Electron.*, vol. 9, no. 5, pp. 571–580, May 1966.
- [5] N. Jankovic, O. Kryvchenkova, S. Batcup, and P. Igić, "High sensitivity dual-gate four-terminal magnetic sensor compatible with SOI FinFET technology," *IEEE Electron Device Lett.*, vol. 38, no. 6, pp. 810–813, Jun. 2017.
- [6] S. Kordic, "Integrated silicon magnetic-field sensors," *Sens. Actuators*, vol. 10, no. 3–4, pp. 347–378, Nov./Dec. 1986.
- [7] F. C. Castaldo, V. R. Mognon, and C. A. dos Reis Filho, "Magnetically coupled current sensors using CMOS split-drain transistors," *IEEE Trans. Power Electron.*, vol. 24, no. 7, pp. 1733–1736, Jul. 2009.
- [8] R. Rodriguez-Torres, E. A. Gutierrez-D., R. Klima, and S. Selberherr, "Three-dimensional analysis of a MAGFET at 300 K and 77 K," in *Proc. 32nd European Solid-State Device Research Conference*, pp. 151–154, 2002.
- [9] M. Meneghini, G. Meneghesso, and E. Zanono, Eds., *Power GaN devices*. Springer, 2017.
- [10] R. Quay, *Gallium nitride electronics*. Berlin: Springer-Verlag, 2008.
- [11] A. Asgari, S. Babanejad, and L. Faraone, "Electron mobility, Hall scattering factor, and sheet conductivity in AlGaIn/GaN heterostructures," *J. Appl. Phys.*, vol. 110, no. 11, p. 113713, Dec. 2011.
- [12] S. Russo and A. Di Carlo, "Influence of the source–gate distance on the AlGaIn/GaN HEMT performance," *IEEE Trans. Electron Devices*, vol. 54, no. 5, pp. 1071–1075, May 2007.
- [13] S. Yagi *et al.*, "High breakdown voltage AlGaIn/GaN MIS–HEMT with SiN and TiO<sub>2</sub> gate insulator," *Solid. State. Electron.*, vol. 50, no. 6, pp. 1057–1061, Jun. 2006.
- [14] O. Aktas, Z. F. Fan, S. N. Mohammad, A. E. Botchkarev, and H. Morkoç, "High temperature characteristics of AlGaIn/GaN modulation doped field-effect transistors," *Appl. Phys. Lett.*, vol. 69, no. 25, p. 3872, Jun. 1998.
- [15] N. Maeda, K. Tsubaki, T. Saitoh, and N. Kobayashi, "High-temperature electron transport properties in AlGaIn/GaN heterostructures," *Appl. Phys. Lett.*, vol. 79, no. 11, pp. 1634–1636, Sep. 2001.
- [16] M. Meneghini, I. Rossetto, D. Bisi, M. Ruzzarin, M. Van Hove, S. Stoffels, T.-L. Wu, D. Marcon, S. Decoutere, G. Meneghesso, and E. Zanoni, "Negative bias-induced threshold voltage instability in GaN-on-Si power HEMTs," *IEEE Electron Device Lett.*, vol. 37, no. 4, pp. 474–477, Apr. 2016.